Validation of Dynamic optical coherence tomography for non-invasive, in vivo microcirculation imaging of the skin

L. Themstrup [a,*], J. Welzel [b], S. Ciardo [c], R. Kaestle [b], M. Ulrich [d], J. Holmes [e], R. Whitehead [e], E.C. Sattler [f], N. Kindermann [b], G. Pellacani [c], G.B.E. Jemec [a]

[a] Department of Dermatology, Zealand University Hospital, Roskilde; Health Sciences Faculty, University of Copenhagen, Denmark
[b] Department of Dermatology and Allergology, General Hospital Augsburg, Augsburg, Germany
[c] Department of Dermatology, University of Modena and Reggio Emilia, Modena, Italy
[d] CMB/Collegium Medicum Berlin, Berlin, Germany
[e] Michelson Diagnostics Ltd., Kent, UK
[f] Department of Dermatology and Allergology, Ludwig-Maximilian University, Munich, Germany

Introduction

The microcirculation plays an important role in the physiological and pathological processes in the skin. The term microcirculation usually refers to arteries, arterioles, capillaries, and venules with a diameter of <150 μm and is essential for oxygenation, nutritional exchange and blood flow regulation of the skin (Roustit and Cracowski, 2013; Eriksson et al., 2014). So far, evaluation of the cutaneous vasculature has primarily been based on either purely functional (e.g. laser Doppler, laser speckle and tissue oxygenation) or strictly morphological techniques (e.g. videodermoscopy) (Ruaro et al., 2016); however, recent technological advances have provided new non-invasive methods for assessing both aspects of the skin microvasculature (Roustit and Cracowski, 2012). One of these methods is based on optical coherence tomography (OCT), which is an emerging technology in dermatology providing high-resolution, real-time microstructural images of the skin to a depth of up to 2 mm. A wide range of skin disorders have been studied with OCT and the capability of OCT to image skin lesions, including non-melanoma skin cancer, is now established (Hussain et al., 2015; Ulrich et al., 2015; Sattler et al., 2013; Boone et al., 2015; Maier et al., 2013) and visualization of vascular structures has been documented (Ring et al., 2013; Pelosini et al., 2013). A novel angiographic

Abbreviations: OCT, optical coherence tomography; D-OCT, Dynamic optical coherence tomography; LSCI, laser speckle contrast imager; SV, speckle variance.

* Corresponding author at: Zealand University Hospital, Department of Dermatology, Sygehusvej 10, 4000 Roskilde, Denmark.
E-mail address: lotte.themstrup@gmail.com (L. Themstrup).

variation of OCT, named "Dynamic OCT" (D-OCT) has recently been developed utilizing the OCT signal to specifically extract information regarding the skin microvasculature (Ulrich et al., 2016). The D-OCT technique is sensitive to the movement of blood cells and thereby obtains integrated information on vascular morphology as well as flow data to a skin depth usually reaching the mid dermis. In recent years the cutaneous vascular circulation has been recognized as an accessible and potentially representative vascular bed to examine the mechanisms of microcirculatory function and dysfunction (Holowatz et al., 2008). D-OCT imaging, providing both functional and morphologic information about the skin microvasculature, therefore has the potential to play an important role in the diagnosis and monitoring of a variety of dermatologic diseases such as vascular diseases, inflammatory skin diseases, wounds and malignant lesions (De Carvalho et al., 2015; Blatter et al., 2012). However, D-OCT has not previously been validated against already accepted blood flow measuring tools. Validation of D-OCT would substantiate its ability to reliably identify changes in the cutaneous vascular networks and give support for further studies on the use of D-OCT in both experimental and clinical settings.

Methods

35 healthy subjects were recruited for the study, which consisted of three experiments. The study was carried out in three European clinical dermatology centres from September 2014 to February 2015; only subjects aged >18 years and without active skin disease were included. The institutional review board of each centre approved the study (SJ-397) and all subjects provided written informed consent in accordance with the Declaration of Helsinki.

In order to validate the D-OCT images against existing techniques for blood flow measuring we performed consecutive D-OCT, chromametry and laser speckle contrast imager (LSCI) measurements on identical skin sites in all of the experiments.

Three experiments were set up to examine the physiologic changes of vascular blood perfusion. To ensure reproducible results from all the clinical centres the study procedures were rehearsed at a joint meeting before the outset of the study. All data from the three study centres was sent to the study coordinator at Zealand University Hospital, Roskilde, Denmark for data analysis. Detailed descriptions of the experiments are reported in the following.

Experiment I. Imaging of blood vessels in the skin during positional changes of the limbs

The subject was placed horizontally on a bed. An area on the ventral side of the wrist on the upper extremity and another area just distal to the medial malleolus on the lower extremity was marked. Chromametry measurements and D-OCT imaging were performed on the marked areas (baseline measurements). Subsequently, the subject was placed standing and the measurements were repeated in the marked skin area distal to the malleolus. The subject's arm was then elevated for 3 min and with the arm in elevated position the measurements were repeated. Following this, the arm was lowered for 2 min and the measurements were repeated. Because LSCI is very sensitive to movement, has a limited reach and requires a black backcloth for imaging it was not possible to perform LSCI flux measurements in this experiment.

Experiment II. Imaging of blood vessels in the skin subjected to vasoactive butoxyethyl nicotinate ointment (FINALGON®)

20 of the 35 subjects participated in this experiment. A round skin area was marked on the ventral side of the wrist. The subjects then received a single thin layer of butoxyethyl nicotinate (BN) ointment (FINALGON®, Boehringer Ingelheim Pharma GmbH & Co. KG, Germany) applied to the marked area. BN is a potent topical rubefacient that produces redness in the skin by causing a dilation of the capillaries. D-OCT images, LSCI and chromametry measurements of the marked skin area were acquired at baseline and 20 min after application of the BN ointment.

Experiment III. Imaging of blood vessels in the skin subjected to vascular occlusion

A round skin area was marked on the dorsum of the hand. A pneumatic cuff was placed around the upper arm and inflated to 30 mm Hg above the systolic blood pressure. After 3 min the occlusion pressure was released. D-OCT images, LSCI and chromametry measurements of the marked skin area were acquired at baseline, during occlusion and 45 s after the release of the occlusion pressure (post-occlusive hyperaemia).

Measurement tools

The main technical specifications of the measurement tools used in this study are presented in Table 1. A short description of the measurement techniques and data analysis used in this study is provided below.

Dynamic OCT

For D-OCT imaging a commercially available OCT scanner was used (VivoSight, Michelson Diagnostics, Kent, UK). The in vivo images of the microcirculation in the skin were acquired using the build-in D-OCT/speckle variance (SV) option in the system. The D-OCT images were acquired by placing the hand-held probe on the skin. The skin surface was not prepared before the OCT scans and there was no off-line post-processing. For the calculation of SV, rapidly repeated OCT scans are acquired in the same location and analysed to detect changes between these successive scans (Mariampillai et al., 2008). A multi-slice scan modality was used consisting of 120 B-scans (in the x-y plane) sep-

Table 1
Technical specifications of the imaging and measurement tools used in the study.

Dynamic OCT (VivoSight)	
Image acquisition	Non-invasive
System type	Multi-beam Swept-Source Frequency Domain
Laser system	1305 nm, class 1
A-line rate	20 kHz
Optical resolution in tissue	**<7.5μm laterally and <5μm axially**
Pixel size	4.44 μm
Voxel size	4.44 x 4.44 x 50.4 μm (for a 120 slice en-face scan)
Field of view	36 mm^2 (6 mm x 6 mm)
Imaging depth "structural" OCT	Tissue dependent, maximum 2 mm
Microvascular imaging depth	~500 μm
Image acquisition	Cross-sectional (vertical) and en-face (horizontal)
Image acquisition time	multislice, 120 B-scans: 30 sec.
Laser Speckle Contrast Imaging (moorFLPI-2)	
Image acquisition	Non-invasive, non-touch
Laser system	785 nm, class 1
Field of view	Up to 15 cm x 20 cm
Imaging depth	Maximum ~1 mm
Image acquisition	Single point, single image, video mode
Image Acquisition Rate	Maximum 25 images per sec.
Measurement units	Flux
Chromametry (CR-400 Chroma meter)	
Measurement acquisition	Non-invasive
Light source	Pulsed xenon lamp
Color system	CIE L*a*b*
Measurement area	8 mm in diameter
Measurement time	8 seconds (mean value of three readings)

arated by 50.4 μm in the y direction. Users already familiar with the specific OCT system performed all of the OCT scans (Themstrup et al., 2016).

Dynamic-OCT data analysis

We used a proprietary software tool (Michelson diagnostics Ltd.) to extract a quantitative measure of the SV-signal in the D-OCT images. The specification of the tool has previously been reported (Themstrup et al., 2016). The average numerical value of the SV-signal from a 0.1–0.35 mm depth interval was calculated for each D-OCT scan and the results were compared.

The morphology and vascular pattern were assessed in horizontal D-OCT images. The same depth was chosen for all images in order to avoid normal anatomical variation in vessel morphology (depth-dependent differences in vasculature). For this we utilized a feature in the 'OCT Analyse' review software (Michelson diagnostics Ltd.) that detects and follows the curved surface of the skin and thereby ensures that the whole area of the horizontal image (36 mm^2) is viewed at the same depth below the skin surface (Themstrup et al., 2016). In order to locate a fitting skin depth for doing standardised evaluations of the vessel morphology, all of the SV measurements from experiment I (upper extremity) were plotted against the depth below the skin surface. From this the maximum slope for each graph was determined, indicating the highest variation in SV signal. The correlated depths were identified and the average depth was calculated to be 0.44 mm below the skin surface. The blood vessels identified at this skin depth are located in the upper/mid part of the dermis. Two of the authors (LT and GJ) performed blinded evaluations of the 320 randomised D-OCT horizontal images, assessing the number of visible vessels (LT), the extent of the vascular pattern (LT and GJ) and the vessel morphology on each frame (LT and GJ). The number of vessels and the extent of the vascular network were categorized on an ordinal scale and the vascular morphology was nominally categorized as either: 1) no recognizable morphology; 2) predominantly coarse vessels; 3) predominantly small vessels; 4) predominantly mixed vessels.

Chromametry

In this study we used the CR-400 Chromameter (Konica Minolta, Inc., Tokyo, Japan) for skin colour measurements based on the CIE L*a*b* colour system. The a* parameter represents changes in redness along a red/green axis (Clarys et al., 2000). The changes in the a* parameter was used as an indirect measure of blood flow changes in the skin. The instrument was calibrated every day using a white calibration plate. Two chromameter measurements (each consisting of the mean value of three readings) were performed each time and a mean was calculated.

Laser speckle contrast imaging (LSCI)

We used the moorFLPI-2 system (Moor Instruments Ltd., Devon, UK) measuring average blood flow velocity and concentration of moving red blood cells in the superficial skin vasculature (Eriksson et al., 2014). LSCI has a fast measurement time, but does not give information on skin vessel morphology. Calibration of the system was performed every 2–4 weeks. We recorded LSCI measurements of the marked areas on the skin over a time period of 30 s. The data was then analysed using moorFLPI review software (Moor Instruments Ltd., Devon, UK) and the average flux in the marked area was calculated for each measurement.

Statistics

A Spearman's rank-order correlation was run to determine the relationship between the LSCI flux measurements and D-OCT SV signal measurements. The Spearman's correlation was used because the LSCI flux data were not distributed normally. Correlation analysis of the normally distributed redness (a*) and D-OCT SV signal data was performed using Pearson's correlation coefficient.

In order to calculate the quantitative difference within each pair of before-and-after intervention measurements, we used the paired samples *t*-test.

For analysing the results from the blinded observer evaluations of number of vessels and extent of network, we used the Wilcoxon signed-rank test to calculate the differences within each pair of before-and-after intervention evaluations (ordinal data; non-parametric). For the analysis of the extent of the vascular network the blinded evaluations from the two authors were checked and if the scores differed with >2 points on the ordinal scale the image was reassessed and consensus was obtained. Reassessments were done in 22 cases (6.9% (22/320)). The mean value of the observers' scores was then calculated and used for conducting the Wilcoxon signed-rank test. The nominally categorized vascular morphology data from the two observers were analysed separately using 4×4 contingency tables and Fisher's exact test in order to test for symmetry (the distribution of vessel morphology before and after intervention). Lastly, Cohen's kappa was performed to measure the inter-rater agreement for the two observers evaluations of vascular morphology. A p-value < 0.05 was regarded as statistically significant. The analyses were carried out using IBM SPSS Statistics for Macintosh version 22.0 (IBM Corp, Armonk, NY, USA).

Results

A total of 35 healthy participants (9 men, 26 women) from three European clinical dermatology centres were included in the study. The median age was 30 years (23–60) and the skin types varied from I–IV on the Fitzpatrick scale.

There was a positive correlation (Spearman's) between the D-OCT SV-signal measurements and the laser speckle flux measurements, which was statistically significant ($r_s = 0.49$; 95% CI [0.36–0.62]; $p < 0.001$), and also the redness a* measurements were positively correlated (Pearson's) with the D-OCT SV-signal measurements ($r = 0.48$; 95% CI [0.41–0.55]; $p < 0.0001$).

The results of the quantitative measurements of blood flow from experiment I, II and III are summarized in Table 2 and illustrated in fig. 1. In experiment 'I' both the redness (a*) and the *D*-OCT SV-signal measurements showed a significant increase in blood flow after positional changes of the arm from an elevated and prone position (baseline) to a lowered position (see Fig. 2). Similar results were found for the positional changes of the lower extremities. Skin blood flow, measured by chromametry (a*), was significantly reduced with the elevation of the arm for 3 min, however the small reduction in SV-signal measured by D-OCT was not statistically significant. In experiment II, all the measurement tools (chromametry, D-OCT and LSCI) showed highly significant quantitative differences in blood flow before and after the application of BN (see Fig. 3). In experiment III there were significant measurable quantitative differences in blood flow before and after the vascular occlusion (see Fig. 4). The measurements of D-OCT SV-signal and the redness a* were not significantly different before and during the vascular occlusion phase although the LSCI flux measurements were able to demonstrate a difference in blood flow.

The results of the blinded observer evaluations of number of vessels and extent of vascular network in the D-OCT images are summarized in Table 3. Except for the experiment with positional change from prone to lowered arm, all of the evaluations showed significant changes in number of vessels and extent of vascular network before and after intervention. The blinded evaluations of the predominant vascular morphology (four categories) in the D-OCT images generally showed no significant changes in the overall distribution of vessel morphology before and after intervention. The summarized results of the blinded observer evaluations of the vascular morphology are shown in Table S1 (Supplementary material). To determine the agreement between the two observers

Table 2
Results of the quantitative measurements of blood flow.

	n[A]	Mean	Mean	Mean difference	95% confidence interval	p-value
Experiment I (positional changes of the limbs)						
Chromametry - a*						
Arm / lowered position	35	prone: 6.48	lowered: 11.03	4.55	3,9 - 5,1	<0,0005
Arm prone position / elevated position	35	prone: 6.48	elevated: 5.07	-1.41	-1.95 - -0,88	<0,0005
Arm elevated position / lowered position	35	elevated: 5.07	lowered: 11.03	5.96	5.2-6.7	<0.0005
Leg prone position / standing position	35	prone: 6.7	standing: 8.02	1.32	0.8 - 1.8	<0.0005
Dynamic OCT - SV signal						
Arm prone position / lowered position	35	prone: 0.1258	lowered: 0.1434	0.018	0.005 - 0.029	0.006
Arm prone position / elevated position	34	prone: 0.1259	elevated: 0,1222	-0.0037	-0.002 - 0.0099	0.224
Arm elevated position / lowered position	34	elevated: 0.1222	lowered: 0.1445	0.022	0.009 - 0.035	0.002
Leg prone position / standing position	35	prone: 0.1295	standing: 0.1399	0.010	0.004 - 0.015	<0.0005
Experiment II (butoxyethyl nicotinate ointment (BN))						
Chromametry (a*) before BN / after BN	20	before: 7.5	after: 12.9	5.4	4.5 - 6.4	<0.0005
Dynamic OCT before BN / after BN	20	before: 0.13	after: 0.23	0.1	0.081 - 0.115	<0.0005
LSCI (flux) before BN / after BN	20	before: 63.2	after: 278.5	215.3	177 - 253	<0.0005
Experiment III (vascular occlusion)						
Chromametry - a*						
Before stasis / stasis	35	before: 10.0	stasis: 10.5	0.45	0.2 -1.1	0.17
Before stasis / hyperaemia	35	before: 10.0	hyperaemia:13.7	3.7	2.9 - 4.5	<0.0005
Stasis / hyperaemia	35	stasis: 10.5	hyperaemia: 13.7	3.25	2.22 - 4.29	<0.0005
Dynamic OCT - SV signal						
Before stasis / stasis	35	before: 0.1425	stasis: 0.1403	-0.00223	-0.0041 - 0.0085	0.47
Before stasis / hyperaemia	35	before: 0.1425	hyperaemia: 0.1688	0.0263	0.017 - 0.03	<0.0005
Stasis / hyperaemia	35	stasis: 0.1403	hyperaemia: 0.1688	0.0285	0.019 - 0.04	<0.0005
LSCI - flux						
Before stasis / stasis	35	before: 47.6	stasis: 18.8	28.8	21.9 - 35.6	<0.0005
Before stasis / hyperaemia	34	before: 47.7	hyperaemia: 70.9	23.2	14.3 - 32.0	<0.0005
Stasis / hyperaemia	34	stasis: 19.02	hyperaemia: 70.9	51.9	41.4 - 62.5	<0.0005

[a] n = number of evaluated cases. A few of the D-OCT images could not be evaluated because of artefacts therefore there is a slight variation in the number of cases.

on the evaluation of vascular morphology Cohen's kappa was performed. There was a fair agreement between the observers (Landis and Koch, 1977) $\kappa = 0.35$, $p < 0.0005$.

Discussion

New technologies must be validated against existing methods when they are introduced, in order to clearly define their advantages and limitations. The comparison of methods validates the results of future investigations using a given method. In this multicenter study we investigated a novel non-invasive imaging tool for assessment of skin vasculature and compared it to LSCI and chromametry, which are tools already validated and accepted for blood flow measuring (Eriksson et al., 2014; Clarys et al., 2000; Bezemer et al., 2010). Overall, our results showed that D-OCT was able to reliably image and identify changes in the skin vasculature consistent with the induced physiological blood flow changes in all three experiments. The quantitative measurements of D-OCT SV-signal were positively correlated to the LSCI flux measurements and to the skin redness a* measurements and in summary, the results of the blinded qualitative observer evaluations of number of vessels and extent of vascular network confirmed the results of the quantitative measurement of blood flow in the D-OCT images. These basic findings support the use of D-OCT imaging for in vivo microcirculation imaging of the skin.

The experiments performed in this study were designed to explore how well D-OCT detected a range of induced physiologic changes in skin blood flow. The results showed that D-OCT imaging was able to identify and quantify both substantial (e.g. application of the potent rubefacient BN) and subtle (e.g. positional changes of the leg) changes in the skin blood flow and that they correlated well with the blood flow changes measured with LSCI and chromametry.

In two settings, the quantitative D-OCT SV-signal measurements did not show the expected changes in blood flow (see Table 2). In experiment I we expected to find a significant reduction in blood flow when the arm was placed in an elevated position compared to the baseline measurements (arm in prone position), but instead the quantitative D-OCT measurements only showed a small reduction in SV-signal not significantly different from the baseline. One of the reasons for this is suspected to be motion artefacts stemming from movements of the subjects during the stage of the experiment that involved elevation of the arm. During the experiment it was difficult to keep the subjects' upper extremity steady in the elevated position and this affected the D-OCT

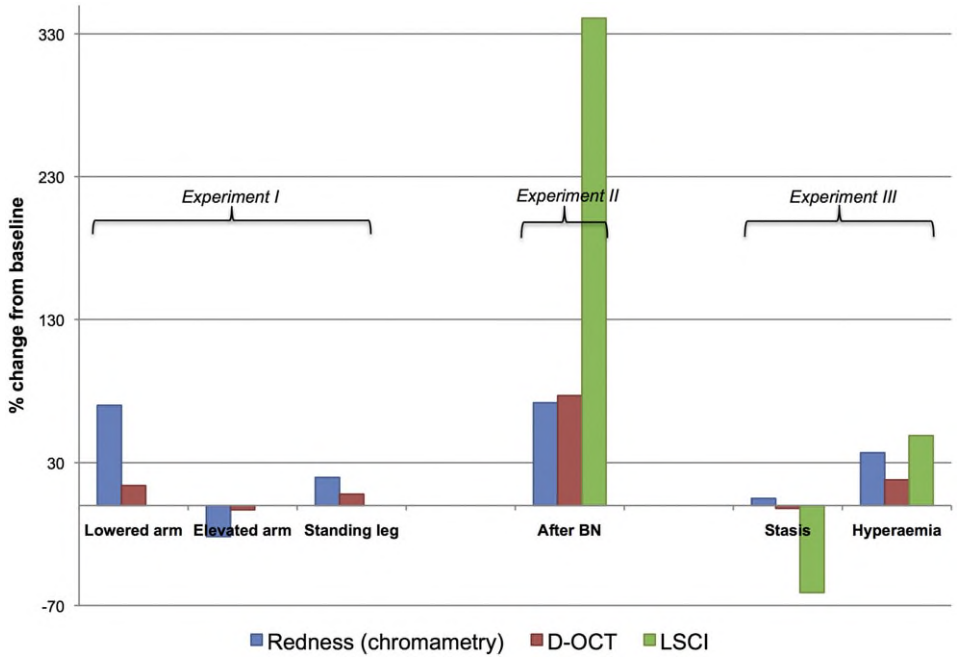

Fig. 1. Chart - quantitative measurements of blood flow expressed in percentage change from baseline. Chart illustration of the results displayed in Table 2 showing the quantitative measurements of blood flow expressed in percentage change from baseline. LSCI: laser speckle contrast imaging, D-OCT: dynamic optical coherence tomography, BN: butoxyethyl nicotinate.

imaging by producing linear horizontal artefacts in the images. The quantitative tool used to measure the SV-signal in the D-OCT images interprets the horizontal artefacts as SV-signal, resulting in a false high measurement of blood flow. However, to the eye, the horizontal linear artefacts can easily be distinguished from the morphologic very different skin vessels. The blinded observer evaluations were therefore able to identify a significant reduction in both number of vessels and extent of vascular network, from baseline to elevated position. In this case, the different results from the SV-signal measurements and manual evaluation of the vessels emphases the advantage of having a tool that provides both quantitative and morphologic information about the blood flow and blood vessels.

In the case of the vascular occlusion experiment (experiment III) the D-OCT and skin redness a* measurements did not show the expected significant decrease in blood flow during the induced stasis. An explanation for this result may be that the D-OCT is sensitive to even quite small movements of red blood cells and that the residual motion of blood cells trapped in the vessels was detected by the D-OCT and not by the LSCI (see Fig. 4). Further studies are needed to explore this. The stagnant blood distal to the tourniquet caused the skin colour to appear slightly reddish or unchanged and therefore the blood flow changes were not evident in the chromameter measurements.

Comparison of D-OCT to LSCI measurements constitutes a reliable way to validate the D-OCT tool for imaging of blood flow in the skin. The LSCI system allows fast measurements of the skin microcirculation with a measuring depth variously reported between 300 μm and a maximum of 1000 μm (Eriksson et al., 2014; Roustit and Cracowski, 2012; Bezemer et al., 2010), making it suitable for dynamic functional tests (Eriksson et al., 2014). By comparison, D-OCT has a depth penetration for vascular imaging in skin of approximately 500 μm, which means that D-OCT and LSCI are both measuring mainly superficial blood flow. Both of the tools have a fast measurement time and are able to detect changes in the skin microcirculation over a short time period, yet unlike LSCI, D-OCT imaging also allows for visual inspection of the vascular morphology, which may offer important additional information regarding which specific structures are responsible for the detected quantitative blood flow changes. The measurements of skin colour performed in this study were included as a crude marker of the induced blood flow changes. The chromameter does not give information about what substances in the skin that generate the colour, but changes on the red/green colour-axis was used as an indirect measure of variations in the blood flow. This makes the skin colour measurements less suitable for comparison to D-OCT than the LSCI measurements, however we chose to include chromametry as a secondary measure because it is robust general objectively quantifiable measurement that could be used to support the concept.

The horizontal D-OCT images allowed us to perform blinded evaluations of different parameters of the vascular morphology including a manual vessel count, the extent of the vascular network and a categorisation of the predominant vascular morphology. The results of the manual vessel count and the evaluation of the extent of the vascular network showed significant identifiable responses to the induced blood flow changes and thereby confirmed the results of the quantitative measurements of blood flow acquired using the LSCI (flux), chromametry (a*) and D-OCT (SV-signal) techniques (Tables 2 and 3).

Generally, D-OCT allowed us to identify the different morphologic vascular changes, based on the anticipated responses to the physiologic experiments. In experiment I the manual vessel count in the D-OCT images on the ventral wrist area showed a slight, but non-significant, increase from baseline to lowered position, however a significant increase in the extent of vascular network could be identified (Table 3). The D-OCT images from the lower extremity showed morphological changes in the vasculature with an increased appearance of predominantly coarse vessels when the leg was placed in a standing position compared to the baseline images (Supplementary material Table S1). This indicates that D-OCT is able to visualise the accumulated blood in the vessels of the lower extremity induced by the gravitational forces when the leg position is changed from prone (baseline) to standing position (Olufsen et al., 2005). In some cases the D-OCT images allowed us to identify and directly compare the exact same vessels at baseline and after intervention. An example of this is seen in Fig. 2 where the D-OCT image shows an increase in the individual vessel diameter and a more coherent extended vascular network when the arm is in a lowered position compared to the baseline image.

The application of the rubefacient BN in experiment II induced prominent changes in the vascular morphology seen in the D-OCT

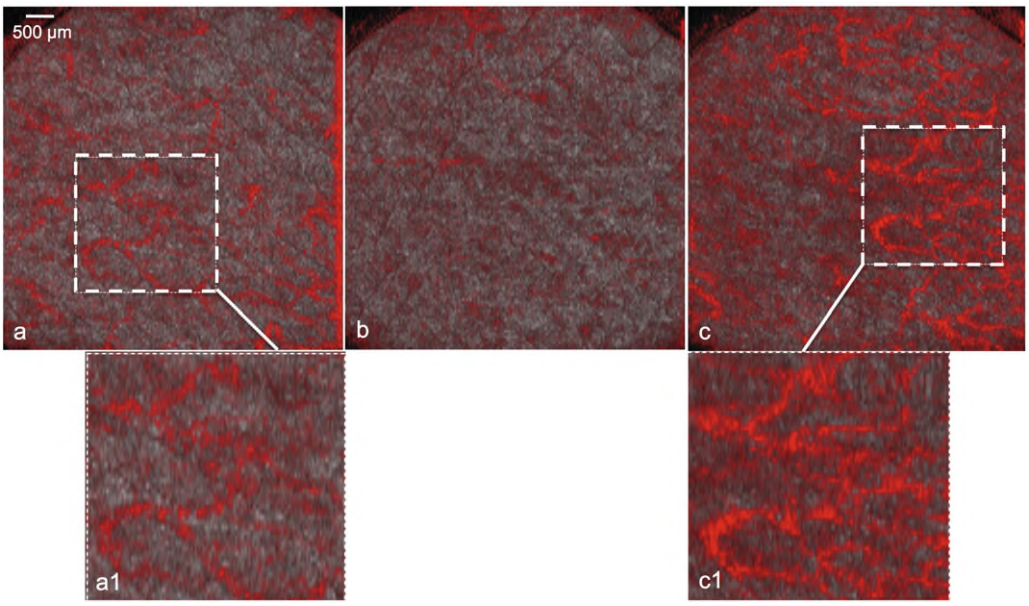

Fig. 2. D-OCT images of ventral wrist during positional changes. Horizontal D-OCT images (original size 6 mm × 6 mm) of skin on the ventral wrist in prone position (a), elevated position (b) and lowered position (c), respectively. The scale bar is applicable to image a, b, and c. Image 'b' shows reduced number of visible vessels when the arm is in an elevated position. Image 'c' shows an increased number of visible vessels when the arm is in a lowered position. Image 'a1' and 'c1' are enlarged clippings of the white dashed areas seen in image 'a' and 'c'. They show the exact same vessels in the D-OCT images both at baseline 'a1' (prone position) and in lowered position 'c1'. In the 'c1' image the vessels seem to have increased in number as well as in diameter.

images where a multitude of predominantly small or mixed calibre vessels appeared in an extended coherent network 20 min after the application of BN (Fig. 3). In experiment III the D-OCT images showed a significant increase in the number of visible vessels as a result of the induced post-occlusive hyperaemia and a general change in morphology towards a predominantly coarse or mixed vascular appearance (Supplementary material Table S1 and Fig. 4).

The blinded observer categorisations of the predominant vascular morphology in the D-OCT images did show some expected changes in the morphologic pattern exemplified above, however the changes in the overall distribution of the vascular morphologic pattern before and after intervention were not statistically significant (Supplementary material Table S1). One explanation for this may be that the changes in the overall morphologic vascular pattern were too subtle to be detected with the naked eye. However, the blinded observers were able to detect the changes in number of vessels and extent of vascular network, so a more likely explanation may be a lack of consensus in describing the normal vascular morphology. Only recently the first investigations

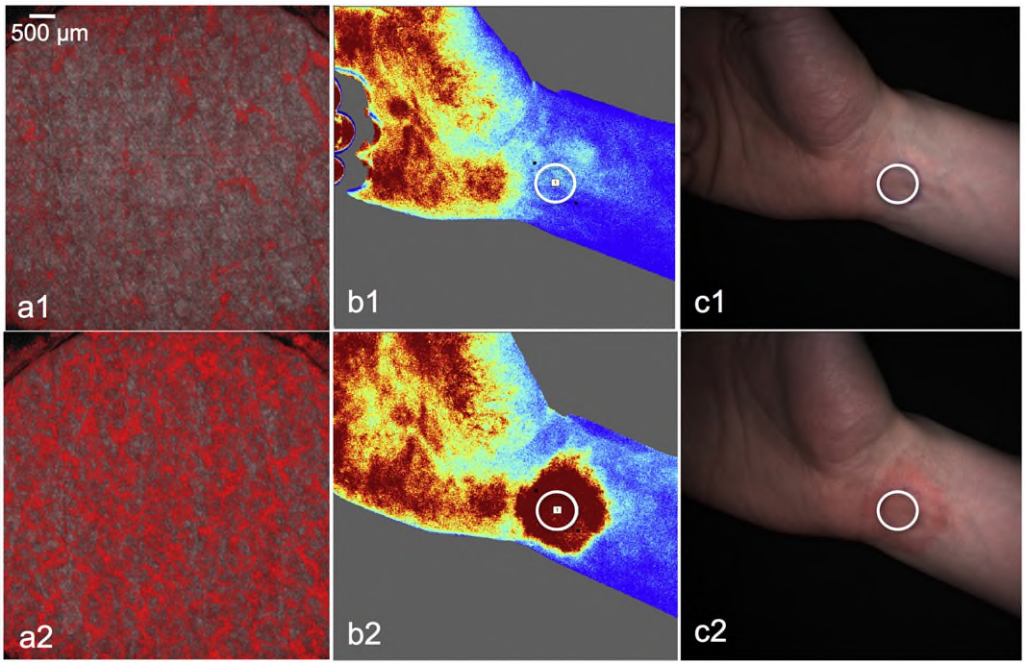

Fig. 3. Images of skin subjected to butoxyethyl nicotinate ointment. The figure shows horizontal D-OCT images (original size 6 mm × 6 mm) (a1 and a2), LSCI images (b1and b2) and clinical photos (c1 and c2) of the ventral wrist before (image row numbered '1') and 20 min after application of topical butoxyethyl nicotinate (image row numbered '2'). The scale bar is applicable to image a1 and a2. The white circles in image in row 'b' and 'c' mark the exact area where the D-OCT images were taken. The images show a significant increase in the number of visible vessels (a2) and redness/blood flow (b2 and c2) 20 min. after the application of butoxyethyl nicotinate.

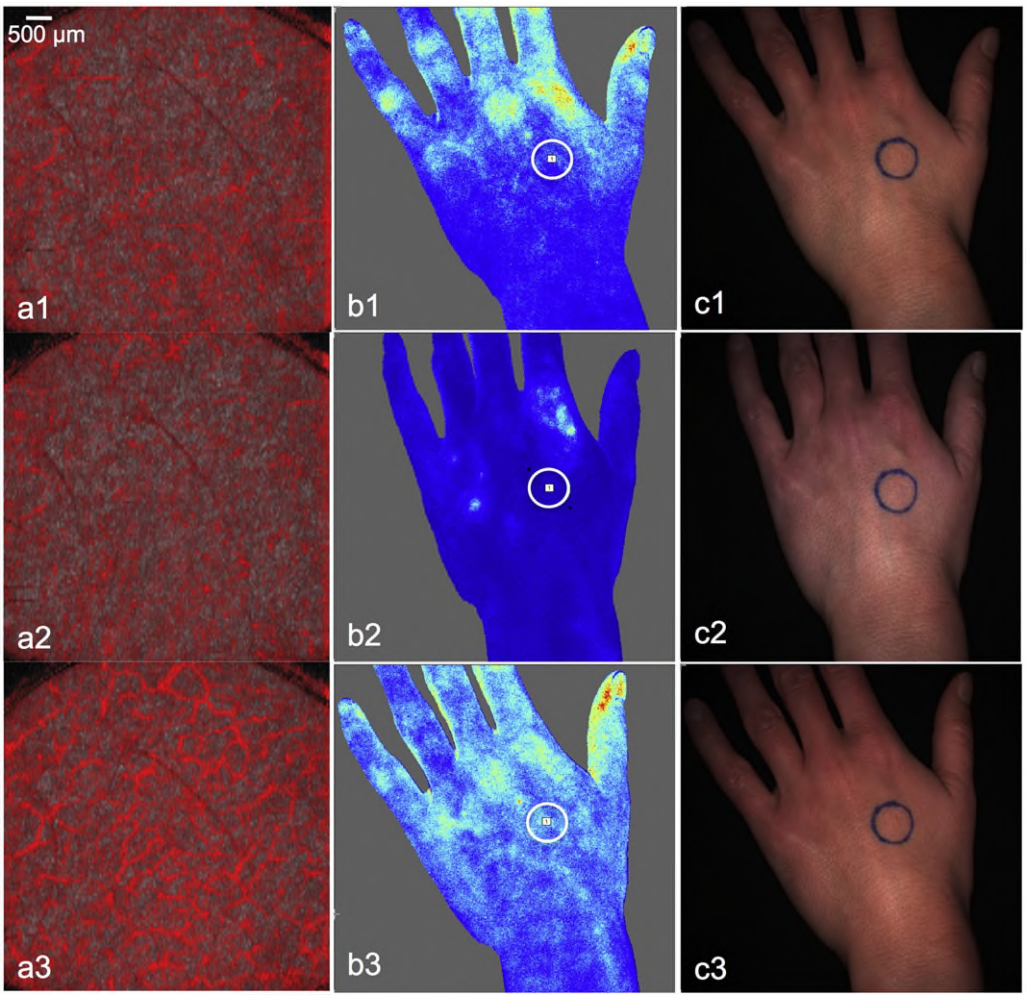

Fig. 4. Images of skin subjected to vascular occlusion and post occlusive hyperaemia. The figure shows horizontal D-OCT images (original size 6 mm × 6 mm) (a1, a2, a3), LSCI images (b1, b2, b3) and clinical photos (c1, c2, c3) of the dorsal hand before (image row number '1'), during (image row number '2') and 45 s. after (image row number '3') vascular occlusions of the arm. The scale bar is applicable to image a1, a2 and a3. The white and black circles in row 'b' and 'c' mark the exact area where the D-OCT images were taken. The images show a significant increase in number of visible vessels (a3) and redness/blood flow (b3 and c3) 45 s. after the release of the occlusion.

have reported on the applicability of D-OCT for the evaluation of pathological vascular patterns (Ulrich et al., 2016; De Carvalho et al., 2015; Themstrup et al., 2016) and being that D-OCT is a novel technique, consensus on clear descriptors of vascular shape and structure in the D-OCT images have not yet been firmly established. The low inter-rater agreement of $\kappa = 0.35$ found in this study is likely to reflect this.

Within the last few years other OCT angiography techniques (Zhang et al., 2015), such as OCT microangiography, have been used for imaging of skin e.g. nail fold capillaries and single cases or case reports of acne lesions, pigmented nevi, scars, wounds etc. (Blatter et al., 2012; Choi et al., 2014a; Baran et al., 2015; Choi et al., 2014b; Gong et al., 2015) and recently OCT based lymphangiography was performed in healthy human skin (Baran et al., 2016). Most of the OCT angiography techniques differ slightly from each other e.g. with respect to number of B-scans at each location and the use of different noise reducing algorithms (Zhang et al., 2015; Choi et al., 2014b). One of the advantages of D-OCT is its ability to capture images of skin vasculature by using a small hand held probe. Other OCT angiography techniques require the probe and the patient to be physically clamped together in order to prevent bulk movement. A hand held probe allows for scans to be acquired at almost any body location and allows the examiner to move more freely around the subject. As with most new medical technologies, their introduction into experimental and clinical medicine is most often incremental and so the ease with which the angiographic OCT images can be acquired may influence how the technology is developed and utilized further on.

In this study we have initiated validation of the use of D-OCT for in vivo microcirculation imaging of the skin by comparison to existing methods primarily by looking at physiological changes. This approach has several advantages: it contrasted the D-OCT results to comparable methods of blood flow measurements; it allowed us to evaluate all of the tools in a controlled experimental set-up and by inducing physiologic changes with a know outcome we could register that D-OCT was able to identify both subtle and more pronounced vascular changes. In addition, the study was carried out in three different centres with different, but identically configured, D-OCT scanners, which also adds to the validity of the results.

Limitations

The study does have limitations. The blood flow measurements of a specific skin area with the three different tools had to be done in rapid succession. The order of the measurement tools was kept consistent in all of the experiments, and although the vascular response to the physiologic changes did not appear to alternate, blood flow fluctuations during the measurement periods cannot be ruled out. Linear, horizontal red artefacts occur in the D-OCT images if the probe is not kept steady during the scanning or if the subject is moving slightly. Especially in experiment I the study set-up made the D-OCT measurements susceptible to motion artefacts and this may have affected the results as previously mentioned. The experimental set-up in experiment I also did not

Table 3
Results of the blinded observer evaluations of the D-OCT images (number of vessels and extent of vascular network).

	n[A]	median | mean	median | mean	z-score	p-value
Experiment I (positional changes of the limbs)					
Number of vessels[1]					
Arm in prone position / lowered position	35	prone: 2 | 2.14	lowered: 2 | 2.40	-0.54	0.59
Arm in prone position / elevated position	35	prone: 2 | 2.14	elevated: 1 | 1.03	-3,27	0.001
Arm in elevated position / lowered position	35	elevated: 1 | 1.03	lowered: 2 | 2.40	-3.47	0.001
Leg in prone position / standing position	35	prone: 1 | 1.03	standing: 1 | 1.63	-2.41	0.016
Extent of vascular network[2]					
Arm in prone position / lowered position	35	prone: 1 | 1.20	lowered: 1 | 1.94	-1.20	0.046
Arm in prone position / elevated position	34	prone: 1 | 1.20	elevated: 0 | 0.57	-2,56	0.010
Arm in elevated position / lowered position	34	elevated: 0 | 0.57	lowered: 1 | 1.94	-3.34	0.001
Leg in prone position / standing position	35	prone: 0 | 0.34	standing: 1 | 0.97	-2.69	0.007
Experiment II (butoxyethyl nicotinate (BN))					
Number of vessels[1]					
Arm before BN / after BN	20	before: 2 | 2.10	after: 5 | 4.30	-3.48	0.001
Extent of vascular network[2]					
Arm before BN / after BN	20	before: 1 | 0.85	after: 6 | 5.05	-3.86	0.0001
Experiment III (vascular occlusion)					
Number of vessels[1]					
Before stasis / stasis	33	before: 2 | 2.46	stasis: 1 | 1.33	-3.51	0.0005
Before stasis / hyperaemia	35	before: 2 | 2.46	hyperaemia: 3 | 3.17	-2.39	0.017
Stasis / hyperaemia	33	stasis: 1 | 1.33	hyperaemia: 3 | 3.17	-3.91	<0.0005
Extent of vascular network[2]					
Before stasis / stasis	35	before: 2 | 1.43	stasis: 0 | 0.60	-3.45	0.001
Before stasis / hyperaemia	35	before: 2 | 1.43	hyperaemia: 2 | 2.34	-2.63	0.008
Stasis / hyperaemia	35	stasis: 0 | 0.60	hyperaemia: 2 | 2.34	-3.84	0.0001

[a] n = number of evaluated cases. A few of the D-OCT images could not be evaluated because of artefacts therefore there is a slight variation in the number of cases.

[b] Number of visible vessels were classified in ordinal categories: 0=no visible vessels; 1=1–5 visible vessels; 2=5–10 visible vessels; 3=10–15 visible vessels; 4=15–20 visible vessels; 5 ≥ 20 visible vessels.

[c] Extent of visible vascular networkwas classified in ordinal categories: 0=no visible vascular network; 1 ≤ 10% of the image area; 2=10–30% of the image area; 3=30–50% of image area; 4 = 50–70% of image area; 5 = 70–90% of image area; 6 ≥ 90% of image area.

allow LSCI measurements. This meant that the D-OCT measurements were only juxtaposed to chromametry, which is not optimal because the skin redness measurements are less comparable to D-OCT than LSCI is. The primary limitation of D-OCT is the limited depth penetration of around 500 μm where signal noise becomes dominant. Therefore, D-OCT is not suitable for measurements of very thick skin, nor can it penetrate to measure the deep vascular dermis. Also, the resolution may be insufficient to detect and measure flow in the finest blood capillaries of the skin (diameter ~ 10 μm) (Themstrup et al., 2016).

Supplementary data to this article can be found online at http://dx.doi.org/10.1016/j.mvr.2016.05.004.

Acknowledgments

The project is part of the ADVANCE project that has received funding from the European Union's ICT Policy Support Programme as part of the Competitiveness and Innovation Framework Programme, grant agreement no: 621015. The manuscript reflects only the author's views and the European Union is not liable for any use that might be made of information contained herein.

We would like to thank Adam Andersen Læssøe, MSc, and Peter Theut Riis, MD, for helping with randomising the data from the study. We thank the Section of Biostatistics at Copenhagen University for statistical advice.

References

Roustit, M., Cracowski, J.L., 2013. Assessment of endothelial and neurovascular function in human skin microcirculation. Trends Pharmacol. Sci. 34 (7), 373–384.
Eriksson, S., Nilsson, J., Sturesson, C., 2014. Non-invasive imaging of microcirculation: a technology review. J. Med. Devices (Auckland, NZ) 7, 445–452.
Ruaro, B., Sulli, A., Pizzorni, C., Paolino, S., Smith, V., Cutolo, M., 2016. Correlations between skin blood perfusion values and nailfold capillaroscopy scores in systemic sclerosis patients. Microvasc. Res. 105, 119–124.
Roustit, M., Cracowski, J.L., 2012. Non-invasive assessment of skin microvascular function in humans: an insight into methods. Microcirculation (New York, NY: 1994) 19 (1), 47-64.
Hussain, A.A., Themstrup, L., Jemec, G.B., 2015. Optical coherence tomography in the diagnosis of basal cell carcinoma. Arch. Dermatol. Res. 307 (1), 1–10.
Ulrich, M., von Braunmuehl, T., Kurzen, H., Dirschka, T., Kellner, C., Sattler, E., et al., 2015. The sensitivity and specificity of optical coherence tomography for the assisted diagnosis of nonpigmented basal cell carcinoma: an observational study. Br. J. Dermatol. 173 (2), 428–435.
Sattler, E., Kastle, R., Welzel, J., 2013. Optical coherence tomography in dermatology. J. Biomed. Opt. 18 (6), 061224.

Boone, M.A., Suppa, M., Pellacani, G., Marneffe, A., Miyamoto, M., Alarcon, I., et al., 2015. High-definition optical coherence tomography algorithm for discrimination of basal cell carcinoma from clinical BCC imitators and differentiation between common subtypes. J. Eur. Acad. Dermatol. Venereol.: JEADV.

Maier, T., Braun-Falco, M., Hinz, T., Schmid-Wendtner, M.H., Ruzicka, T., Berking, C., 2013. Morphology of basal cell carcinoma in high definition optical coherence tomography: en-face and slice imaging mode, and comparison with histology. J. Eur. Acad. Dermatol. Venereol.: JEADV 27 (1), e97–104.

Ring, H.C., Mogensen, M., Banzhaf, C., Themstrup, L., Jemec, G.B., 2013. Optical coherence tomography imaging of telangiectasias during intense pulsed light treatment: a potential tool for rapid outcome assessment. Arch. Dermatol. Res. 305 (4), 299–303.

Pelosini, L., Smith, H.B., Schofield, J.B., Meeckings, A., Dhital, A., Khandwala, M., 2013. In vivo optical coherence tomography (OCT) in periocular basal cell carcinoma: correlations between in vivo OCT images and postoperative histology. Br. J. Ophthalmol. 97 (7), 890–894.

Ulrich, M., Themstrup, L., de Carvalho, N., Manfredi, M., Grana, C., Ciardo, S., et al., 2016. Dynamic optical coherence tomography in dermatology. Dermatology.

Holowatz, L.A., Thompson-Torgerson, C.S., Kenney, W.L., 2008. The human cutaneous circulation as a model of generalized microvascular function. J. Appl. Physiol. (Bethesda, Md: 1985) 105 (1), 370–372.

De Carvalho, N., Ciardo, S., Cesinaro, A., Jemec, G., Ulrich, M., Welzel, J., et al., 2015. In vivo micro-angiography by means of speckle-variance optical coherence tomography (SV-OCT) is able to detect microscopic vascular changes in naevus to melanoma transition. J. Eur. Acad. Dermatol. Venereol.: JEADV.

Blatter, C., Weingast, J., Alex, A., Grajciar, B., Wieser, W., Drexler, W., et al., 2012. In situ structural and microangiographic assessment of human skin lesions with high-speed OCT. Biomed. Opt. E. 3 (10), 2636–2646.

Mariampillai, A., Standish, B.A., Moriyama, E.H., Khurana, M., Munce, N.R., Leung, M.K., et al., 2008. Speckle variance detection of microvasculature using swept-source optical coherence tomography. Opt. Lett. 33 (13), 1530–1532.

Themstrup, L., Ciardo, S., Manfredi, M., Ulrich, M., Pellacani, G., Welzel, J., et al., 2016. In vivo, micro-morphological vascular changes induced by topical brimonidine studied by dynamic optical coherence tomography. J. Eur. Acad. Dermatol. Venereol.: JEADV.

Clarys, P., Alewaeters, K., Lambrecht, R., Barel, A.O., 2000. Skin color measurements: comparison between three instruments: the Chromameter(R), the DermaSpectrometer(R) and the Mexameter(R). Skin Res. Technol. 6 (4), 230–238.

Landis, J.R., Koch, G.G., 1977. The measurement of observer agreement for categorical data. Biometrics 33 (1), 159–174.

Bezemer, R., Klijn, E., Khalilzada, M., Lima, A., Heger, M., van Bommel, J., et al., 2010. Validation of near-infrared laser speckle imaging for assessing microvascular (re)perfusion. Microvasc. Res. 79 (2), 139–143.

Olufsen, M.S., Ottesen, J.T., Tran, H.T., Ellwein, L.M., Lipsitz, L.A., Novak, V., 2005. Blood pressure and blood flow variation during postural change from sitting to standing: model development and validation. J. Appl. Physiol. (Bethesda, Md: 1985) 99 (4), 1523–1537.

Zhang, A., Zhang, Q., Chen, C.L., Wang, R.K., 2015. Methods and algorithms for optical coherence tomography-based angiography: a review and comparison. J. Biomed. Opt. 20 (10), 100901.

Choi, W.J., Wang, H., Wang, R.K., 2014a. Optical coherence tomography microangiography for monitoring the response of vascular perfusion to external pressure on human skin tissue. J. Biomed. Opt. 19 (5), 056003.

Baran, U., Choi, W.J., Wang, R.K., 2015. Potential use of OCT-based microangiography in clinical dermatology. Skin Res. Technol.

Choi, W.J., Reif, R., Yousefi, S., Wang, R.K., 2014b. Improved microcirculation imaging of human skin in vivo using optical microangiography with a correlation mapping mask. J. Biomed. Opt. 19 (3), 36010.

Gong, P., Es'haghian, S., KA, H., Murray, A., Rea, S., BF, K., et al., 2015. Optical coherence tomography for longitudinal monitoring of vasculature in scars treated with laser fractionation. J. Biophotonics.

Baran, U., Qin, W., Qi, X., Kalkan, G., Wang, R.K., 2016. OCT-based label-free in vivo lymphangiography within human skin and areola. Sci. Rep. 6, 21122.